

Surface State Engineering Using Bulk-Band Geometric Phases: Band Inversion and its Observable Implications in One-Dimensional Photonic Crystals

Nitish Kumar Gupta^a, Aditi Chopra^b, Mukesh Kumar^b, Anjani Kumar Tiwari^c, Sudipta Sarkar Pal^{b*},
Harshawardhan Wanare^{a,d} & S Anantha Ramakrishna^{b,d}

^aCentre for Lasers and Photonics, Indian Institute of Technology Kanpur, Kalyanpur, Kanpur -208 016, India

^bCSIR - Central Scientific Instruments Organisation, Chandigarh-160 030, India

^cDepartment of Physics, Indian Institute of Technology–Roorkee, Uttarakhand-247 667, India

^dDepartment of Physics, Indian Institute of Technology Kanpur, Kalyanpur, Kanpur -208 016 India

Received 15 October 2022; accepted 12 June 2023

This work comprehensively investigates possibilities of surface states realization in one-dimensional photonic systems that are terminated with ε -negative and μ -negative bandgap materials. We begin by first fathoming the topological properties of photonic band structure and notice that its bulk properties completely characterize the surface phenomena in all the foreseeable cases. This approach is inspired from topologically non-trivial behavior in low-dimensional condensed matter systems and the ensuing emergence of topologically protected edge states in such systems. Specifically, we will be following the setup of Su-Schrieffer-Heeger model and emulate the topological phenomena in one-dimensional photonic systems with a substantial advantage of relatively less demanding fabrication. More importantly, being distributed systems, the photonic crystal realizations in question further enrich the available parameter space and provide application avenues for topological phenomena. For example, unlike the atomic chains, in the case of photonic crystals, we can achieve the band inversion and topological phase transition without altering the arrangement of constituents. Our investigations primarily focus on exploiting this very aspect of higher-order photonic bandgaps and in this process, we experimentally demonstrate that the bulk-band geometric phases offer a deterministic yet customizable route for surface state engineering.

Keywords: Geometric phase; Photonic bandgap; Photonic crystal; Surface impedance

1 Introduction

Although the importance of topological properties in realizing the novel states of matter were highlighted by Thouless *et al.* in their seminal work pertaining to fermionic systems¹, the universality of topological physics was established only when these ideas were extended to bosonic systems as well²⁻⁴. Notwithstanding their relatively recent discovery, the photonic realizations of topological phases in condensed matter systems have gained significant research interest in the last decade, not only as one of the most active research areas in optics and photonics but also as a catalyst for progress in topological physics at large. From an application viewpoint, we notice that although the photonic analogs of topological materials were conceived partly to facilitate the discovery of fundamental novel phenomena by circumventing some of the technological and control limitations of studying

them in electronic systems; over a while, the research in the domain is primarily driven by the peculiar capabilities they offer to a plethora of light transportation and light-matter interaction avenues⁵⁻²². Many recent explorations of photonic topological insulators establish their application potential in three crucial areas of research: (1) In developing quantum circuitry, (2) In developing topological lasers, and (3) for robust communication on integrated photonic chips. Out of these research areas, the first and the last fields are deeply related, where intense efforts have been made to realize fabrication conducive topological photonic waveguides. While for the second research area of realizing lasing in topologically non-trivial systems, some significant advancements in this direction have been made of late²³⁻²⁵.

Catering to these broad research directions, our work focuses on materializing zero-dimensional topological bound states in one-dimensional photonic systems which are characteristically similar to the

*Corresponding author: (E-mail: sudipta@csio.res.in)

topological edge states observed in a Su-Schrieffer-Heeger atomic chain²⁶. These zero-dimensional photonic states can prove to be instrumental not only in developing sources of radiation with peculiar emission characteristics, but their systematic investigation also provides a fundamental understanding regarding the bound states in general. The origins of these states lie in the non-trivial topological characteristics of their bulk photonic band structure, the details of which can be found in the following references^{27,28}. As far as their experimental realizations are concerned, in this work, we will be using the template of one-dimensional photonic crystals for their materialization. Being a distributed system, the photonic crystal (PhC) realizations not only enrich the available parameter space but also significantly advance the possibilities associated to the Su-Schrieffer-Heeger (SSH) model. For example, unlike the SSH model, photonic crystal realizations permit us to define a fractional composition parameter based on which we can achieve the band inversion and topological phase transition without altering the arrangement of materials in the photonic crystals. This methodology has been efficiently utilized in one of our recent works to realize electro-optically induced dynamic topological phase transitions at the fifth-order bandgap²⁹. In this work also, we will be primarily utilizing the recipe mentioned in²⁹ to realize topologically distinct phases of PhCs and exploit them for explicitly controlling the very existence of surface states.

2 PhC Configuration and Structural Details

To make the upcoming discussions regarding analytical calculations, numerical simulations, and experimental observations more traceable, we explicitly define the PhC configuration and structural details at the very beginning.

All the calculations and experiments in this work are performed on 1-D binary PhC with spatial inversion symmetric (SIS) unit-cell configuration. A representative schematic of PhC is provided in Fig. 1, with the SIS unit-cell being marked with dashed lines. The binary PhC is experimentally fabricated from silicon dioxide (SiO_2) and titanium dioxide (TiO_2) thin films whose optical constants have been determined by spectroscopic ellipsometry. To this objective, we have grown nanometric thin films of TiO_2 and SiO_2 on BK7 glass and sapphire substrates and measured their ellipsometric parameters, from which the optical constants of the thin films have been ascertained. The reference axes have also been

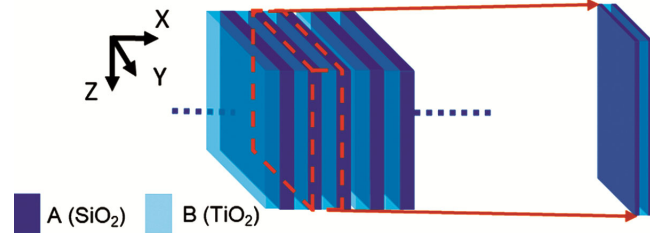


Fig. 1 — Schematic for a SIS binary PhC depicting unit cell configuration and coordinate axes convention.

marked in the schematic; throughout this work the PhC periodicity and the propagation direction is assumed to be along the X-axis. We also consider that the electric and magnetic fields are oriented along Z and Y-axes, respectively.

Finally, we explicitly mention that most of our discussion will be focused on investigating the two topologically distinct PhCs configurations corresponding to

- (1) $\alpha = 0.35$ (Case-1), and
- (2) $\alpha = 0.65$ (Case-2).

Where the parameter α defines the fractional composition of the PhC unit cell and will be discussed in detail in Section 6.

3 Genesis of Surface States in 1-D Photonic Systems

It has been well documented in the existing literature that when an SSH chain is terminated properly (*i.e.*, in the topologically non-trivial configuration), it leads to the appearance of edge states. Likewise, an edge state emerges when two semi-infinite SSH chains of complementary topological characteristics are concatenated. These occurrences are nothing but a manifestation of the bulk-boundary correspondence principle which establishes a formal connection between the bulk topological behavior and surface characteristics.

Coming to classical electromagnetic wave systems, it has been realized that the principles of topological band theory can very well be extended to such systems²⁻⁴. Working along this parallel, we will demonstrate that, like the termination of an SSH chain, if we terminate a PhC (by a trivial photonic insulator of any kind), the possibility of conditional emergence of surface states arises. Since, in the case of 1-D PhCs, their transverse extent is infinite, it is more appropriate to refer to such states as surface states (rather than edge states or bound states). In the coming sections, we will show that just like their fermionic counterparts, the emergence of such surface

states can be appreciated based on the bulk-boundary correspondence principle, however, in the case of photonic realizations, their existence can be understood in highly simplistic terms by referring to the well-known conjugate impedance matching condition (notice here that the character of the surface impedance gets decided by the topological properties of the band structure only). We explain this aspect in some details hereafter: Surface impedance is a concept peculiar to electromagnetics, which is extensively employed to understand the coupling of incoming radiation to an electromagnetic structure or vice-versa. The critical thing to note is that it can be used to proclaim an existence condition for the surface states. The condition has its origins in the reflectionless coupling of incoming radiation to a structure where impedance matching is a must requirement. However, if the structure exhibits a bandgap, the mentioned condition can be tweaked into a conjugate impedance matching condition²⁷ that can predict the existence of the surface state. As per this condition, a perfect surface state emerges at the interface of two semi-infinite media if the sum of their surface impedances on the left and right of the interface is zero. We want to also mention here that the conjugate impedance matching condition mostly comes into picture for bandgap materials as their impedance is reactive.

In later sections, we will show that the sign of (reactive) surface impedance of bandgap materials can be deterministically ascertained only by referring to the bulk-band topology, which signifies a topological origin to this conjugate impedance matching condition of surface states.

4 Theoretical Ascertainment of Bulk Topological Characteristics in 1-DPhC and a Deterministic Route for Topological Phase Transition

The relevant schematic has already been presented in Fig. 1 where we consider a 1-D PhC structure with perfect periodicity in X-direction. For its analysis, we resort to the standard transfer-matrix method³⁰ and work with the unit cell translation matrix under Bloch periodic boundary conditions. Using this formulation, the eigenvalues of the Bloch periodic unit cell translation matrix can be obtained in terms of the matrix coefficients³⁰. Furthermore, the dispersion of the Bloch wave number (K) can also be obtained in terms of matrix coefficients. For brevity, here we only provide the expression for the dispersion relation²⁸

$$\begin{aligned} \cos(K\Lambda) &= \cos(k_a d_a) \cos(k_b d_b) \\ &\quad - \frac{1}{2} \left(\frac{Z_a}{Z_b} + \frac{Z_b}{Z_a} \right) \sin(k_a d_a) \sin(k_b d_b) \end{aligned} \quad \dots(1)$$

where k_a, k_b denote the wave number in layers A and B; Z_a, Z_b denote the impedance for medium A and B; d_a, d_b denote the thicknesses of layers A and B; Λ denotes the physical thickness of unit cell ($\Lambda = d_a + d_b$), and K denotes the Bloch wave number. This equation defines the band structure for 1-D PhC. The absolute value of the right-hand side (RHS) of the Eq. 1 assigns the frequency regions corresponding to the bands and bandgaps. When it is smaller than or equal to unity, the equation gets satisfied for a real value of Bloch momentum K , and the corresponding solutions are the propagating modes defining a passband. On the contrary, if the absolute value of the RHS is greater than unity, only imaginary values of K can satisfy the equation leading to exponentially decaying states denoting a bandgap. Using this formulation, later on we will plot the band structures for two PhC configurations.

For ascertainment of the topological characteristics of the band structure, we resort to geometric Berry phase calculations, which in a 1-D system manifest as geometric Zak phase, defined as²⁷:

$$\theta_n^{Zak} = \int_{-\pi/\Lambda}^{\pi/\Lambda} \left(i \int_{unitcell} dx \epsilon(x) u_{n,K}^*(x) \frac{\partial}{\partial K} u_{n,K}(x) \right) dK \quad \dots(2)$$

With the help of this expression, we can calculate the geometric phases corresponding to each of the isolated bulk-band of the photonic band structure in the first Brillouin zone and thus recognize the topological structure of Bloch eigen functions. Having these ingredients in place, the last task is to relate the geometric phase evolution with the bandgap characteristics, which will be taken up in the next section.

5 Correspondence between Bulk & Surface Characteristics of PhC and Topological Protection of Surface States

In this section, we will be transitioning from bulk characteristics to surface characteristics; in other words, we will ponder upon the bulk-boundary correspondence principle and the ensuing topological protection of surface states (upon proper termination).

Often in topological investigations, we come across the application of the bulk-edge correspondence principle/bulk-boundary correspondence principle. A statement for it in the context of condensed matter systems can be given as: when we bring in two materials with differing topological invariants in physical contact with each other, there must appear an edge state which is spatially localized at the boundary, with its energy lying inside the energy gap of surrounding materials. Without diving into rigorous discussions, the main implications of this principle in case of electromagnetic systems can be understood in a simple and intuitive manner, as follows: in the case of homogeneous media, its bulk properties, such as refractive index, permittivity, or permeability, govern the propagation of electromagnetic waves across the medium. However, if we bring in the aspects of in-coupling or out-coupling of electromagnetic waves traveling to or from this medium to the ambient, these are governed by the surface characteristics, namely, the surface impedance seen by the electromagnetic wave (in other words, the surface impedance governs the scattering of electromagnetic waves upon encountering an interface). As per the bulk-boundary correspondence, these bulk and surface properties are interdependent such that the deduction of one from the other is possible; furthermore, any change in the bulk properties is accompanied with a corresponding emergence of midgap states at the surface. Coming to the case of non-homogeneous media (such as photonic crystals), all the necessary information about the medium characteristics resides in its topological band structure, and in this case, again, there persists a connection between the bulk-band topological properties and the surface properties of the PhC (*i.e.*, surface impedance corresponding to a bandgap). Particularly, in the case of 1-D PhC, this connection has been recently established by proving an interrelationship between the bulk-band Zak phases and the sign of surface impedance²⁷. As per this analysis, for any n^{th} bandgap, its surface impedance sign information can be traced by referring to the evolution of the cumulative bulk-band Zak phases in the following manner:

$$\text{sgn}[\xi^{(n)}] = (-1)^n (-1)^l \exp\left(i \sum_{m=0}^{n-1} \theta_m^{\text{Zak}}\right) \quad \dots (3)$$

where $\xi^{(n)}$ is defined as $i\xi^{(n)} = \frac{Z^{(n)}}{Z_0}$, here $Z^{(n)}$ is the surface impedance of the n^{th} band gap while Z_0 is the

vacuum impedance. This expression establishes a formal connection between the bulk properties of PhC (Zak phases) and the surface characteristics of PhC bandgap (surface impedance). Evidently, any change in the bulk properties of PhC will lead to a corresponding impact on the surface impedance of the bandgap.

Having identified the avenues and methodology to recognize the correspondence between the bulk and surface characteristics, we now turn toward understanding the conditions for surface state existence in PhCs. As mentioned previously, precedence to such investigations is well versed in quantum systems, where it is known that a surface state emerges upon concatenation of two semi-infinite media of differing topological invariants. Here in case of photonic systems we see that the two topologically distinct PhCs lead to complementary surface impedance character, which upon satisfaction of conjugate impedance matching condition lead to the emergence of surface state. From Eq. 3, we notice that the sign of reactive impedance inside the bandgap is solely determined by the evolution of cumulative Zak phases. This realization permits us to equivalently say that Eq. 3 can be employed for determining the existence of surface states (more specifically, any change in the sign of $\xi^{(n)}$ should lead to an emergence of the surface state). Thus, the bulk-band geometric phases and the bandgap surface characteristics are connected and are solely responsible for determining the existence of surface states.

Before concluding this section, we highlight that the surface states in question originate upon proper termination of PhC by a trivial photonic insulator or by a PhC of opposite topological character. In this work, we will be concerned only with the cases where we terminate the PhC with trivial photonic insulators (ϵ -negative or μ -negative-type homogeneous materials). With such terminations, we will demonstrate that existence conditions of surface states become complementary.

6 Band structure Engineering for Discretionary Realization of Surface States

As a culmination of all the discussions of previous sections, we now resort to band structure engineering and judicious application of Eq. 2 and 3 to design PhCs with complementary topological characters at their second-order bandgaps. Thereafter, we terminate these PhCs with trivial photonic insulators to witness

the emergence of conditional surface states. We will be providing results for both possible termination scenarios, *i.e.*, with ε -negative materials and μ -negative materials in simulations. The experimental results are provided, however, only for the ε -negative termination case and not for the μ -negative case as no naturally occurring material offer μ -negative response at optical frequencies (such response can only be artificially produced using metamaterials).

To commence our journey, we require photonic bandgaps with distinct topological characters. In one of our recent works, we have transcribed a routine for band structure engineering and mentioned a straightforward prescription for realizing a change in the topological character by evolving the system across a bandgap closing point²⁹. Two means for such a realization were stated, one based on the unit cell composition variation by virtue of thickness variations and the other based on refractive index modulation. Here, in favour of relatively less demanding experimental realization, we select the method of unit cell composition variation and define a fractional composition parameter

$$\alpha = \frac{n_A d_A}{n_A d_A + n_B d_B} = \frac{n_A d_A}{\gamma} \quad \dots(4)$$

where n_i and d_i denote the refractive indices and layer thicknesses respectively and γ denotes the unit cell optical thickness. Variation in α can effectuate a change in the momentum-space topology of Bloch eigenfunctions associated with higher-order bands, which also leads to a change in the topological character of the corresponding bandgaps. For detailed understanding of genesis of these topological transitions, we suggest the reader to please refer to references²⁷⁻³². Here we will only utilize the recipes mentioned in these references to promulgate two PhC designs with complementary topological character³¹. Specifically, we work around the second-order bandgap of spatial inversion symmetric (SIS) binary photonic crystal (comprising of SiO₂ and TiO₂ with $\gamma = 568\text{nm}$); leading to the two PhC designs with topologically in equivalent second-order bandgaps corresponding to $\alpha = 0.35$, and $\alpha = 0.65$, respectively.

Now before proceeding forward, we need to theoretically establish the opposite topological characters of the second-order bandgaps for these two designs. To this objective, first of all, we perform the calculations for an infinitely periodic SIS 1D PhC

using Eq. 1 and plot the band structures for $\alpha = 0.35$ (Fig. 2: case-1) and $\alpha = 0.65$ (Fig. 2: case-2). To ascertain the topological structure of the bulk-bands, we employ Eq. 2 and calculate the geometric Zak phase for each of the bulk-bands for the two designs. These calculated Zak phases have been depicted alongside the corresponding bands in the band structure plots of Fig. 2. They evidently reveal that as we move from case-1 to case-2, a redistribution of the Zak phases takes place for the neighboring bands. Courtesy to Eq. 3, this must lead to a sign reversal in the surface impedance of the second-order bandgap. The results of these calculations have been explicitly embodied in Fig. 2 by color-coding the bandgaps. From this color-coded band structure, we can see that the surface impedance of the second-order bandgap reverses its sign (color) as we evolve the system from Case-1 to 2. In this manner, we have theoretically proven the authenticity of our proposition that $\alpha = 0.35$ and $\alpha = 0.65$ designs have opposite topological character for the second-order bandgap.

7 Surface State Realization by ε -Negative (ENG) Material Termination: Simulation Results

Having theoretically established the opposite character of second-order bandgaps for Case-1 and Case-2 designs, in this section, we show that conditional surface can be manifested in the present scenario upon terminating the PhCs with trivial photonic insulators. For their demonstration, we come

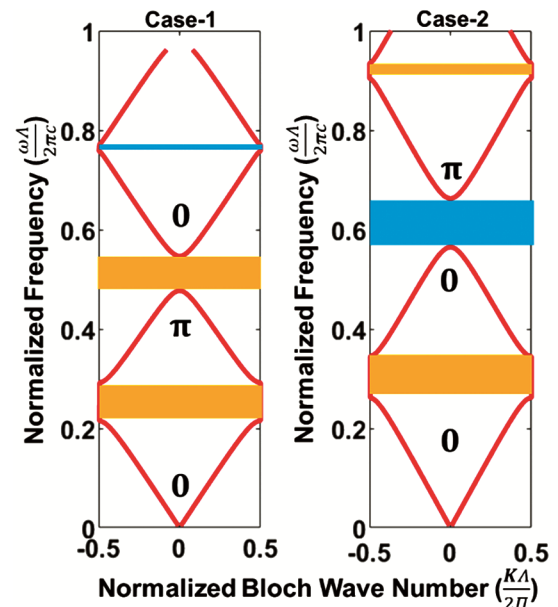


Fig. 2 — Folded bandstructure of PhC with inversion symmetric unit cell for two topologically distinct cases corresponding to $\alpha = 0.35$ (case-1), and $\alpha = 0.65$ (case-2).

back to the designs corresponding to Case-1 and Case-2 and simulate their reflectance performance for four-unit cells using the standard transfer matrix method simulations. The results of these simulations are provided in Fig. 3(a) and Fig. 4(a) (corresponding to Case-1 and Case-2, respectively). Thereafter, we terminate both these finite-size PhCs with an ENG type trivial insulator. This is a realizable scenario as many noble metals exhibit ENG response at optical frequencies, hence, in our demonstrations we will be using a silver film of 40nm thickness as an ENG material. Upon termination, we again resort to TMM simulations to ascertain the spectral reflectance profile, the results of which are plotted in Fig. 3(b) and Fig. 4(b). Evidently, we can see that for this metal terminated PhC a resonating surface state emerges inside the second-order bandgap only for Case-2 PhC (Fig. 4(b)) while no such state appears for Case-1 PhC

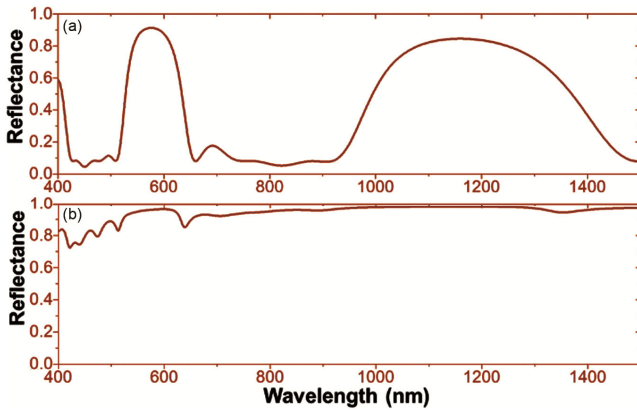


Fig. 3 — (a) TMM Simulated normal incidence reflectance spectrum corresponding to Case-1 PhC design; (b) TMM Simulated normal incidence reflectance spectrum for ENG terminated Case-1 PhC design.

(Fig. 3(b)). Consequently, we can deduce that only the Case-2 PhC design leads to the formation of surface state (at the second-order bandgap) with an ENG-type trivial photonic insulator.

8 Experimental Realization of Surface States by ϵ -Negative Material (metal) Termination

To ascertain the veracity of simulation results, we have fabricated one of the PhC samples (corresponding only to the interesting scenario of Case-2) using the ion assisted electron-beam evaporation system (Evatec AG: BAK761). The fabrication of SiO₂ and TiO₂ layers was performed at a working pressure of 2×10^{-4} mbar having argon and oxygen flow rates of 20 sccm and 8 sccm, respectively. During deposition, the ion source current was maintained at 3.2 Amps. at a potential difference of 120 Volts. Under these fabrication conditions, the deposition rates of 0.5 nm/sec and 0.2 nm/sec were achieved for SiO₂ and TiO₂ (obtained from quartz crystal thickness monitor).

Thereafter the spectral reflectance performance of the sample was measured from a visible-NIR range spectrophotometer at near-normal incidence, as depicted in Fig. 4(c). As a next step, a 40nm silver film (acting as a trivial ENG material) was coated on the sample again the spectral reflectance performance was measured again that is provided in Fig. 4(d). From this plot we can witness the emergence of a surface state in the middle of the second-order bandgap of PhC sample (roughly at 510nm) upon termination with a metal film.

Furthermore, to ascertain the surface state nature of the observed resonating state, in Fig. 5, we plot the

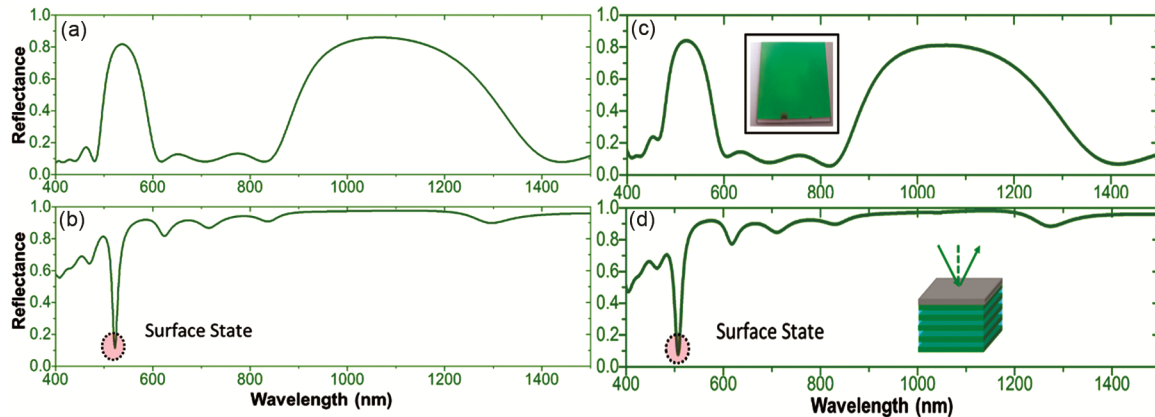


Fig. 4 — (a) TMM Simulated normal incidence reflectance spectrum corresponding to Case-2 PhC design; (b) TMM Simulated normal incidence reflectance spectrum for ENG terminated Case-2PhC design;(c) Measured near-normal incidence reflectance spectrum corresponding to Case-2 PhC design (inset depicts an optical image of the sample); (d) Measured near-normal incidence reflectance spectrum for ENG terminated Case-2 PhC.

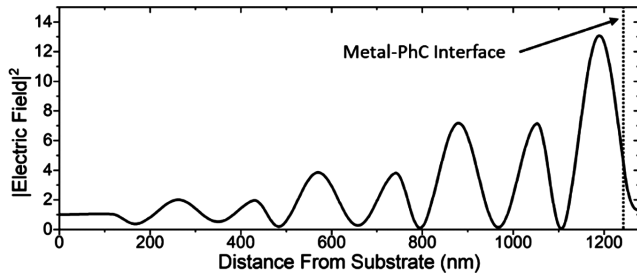


Fig. 5 — Calculated electric field profile across the metal terminated Case-2 PhC structure corresponding to the resonating state of Figure 4.

simulated electric field profile inside the metal terminated PhC structure at the resonance condition. From this plot we can notice the exponential decay of fields (or field envelopes) away from the metal-PhC interface.

9 Surface State Realization by μ -Negative (MNG) Material Termination: Simulation Results

In the previous sections, we have demonstrated the existence/non-existence of the surface states when we properly terminate the PhC with an ENG material. In order to exhaust all the possibilities of termination by a trivial photonic insulator material, in this section, we perform simulations for the scenario when PhC designs are terminated by an MNG-type trivial photonic insulator. A caveat emptor before we begin: this is a hypothetical scenario as none of the naturally occurring materials exhibit MNG response at optical frequencies (although an MNG response can be artificially engendered by resorting to metamaterials). Consequently, we will be providing only simulation results here.

Once again, we start with the Case-1 and Case-2 designs and terminate both these finite-size PhCs with an MNG material having unity relative permittivity and a constant relative permeability of $\mu_r = -10 + 0.5i$ (this is roughly the same numeric value that silver exhibits for its permittivity at 550nm). The thickness of the MNG terminating layer has been taken to be 40nm, and the TMM simulations are performed for the structure, with results depicted in Fig. 6. We notice that while for the MNG-terminated Case-1 PhC surface states appear in both the first-order and the second-order bandgaps (Fig. 6(a)), for the MNG-terminated Case-2 PhC surface state appears only inside the first-order bandgap (Fig. 6(b)). These responses are in stark contrast to those appearing in Fig. 3(b) and Fig. 4(b), respectively where we notice that only the Case-1 PhC design leads to the

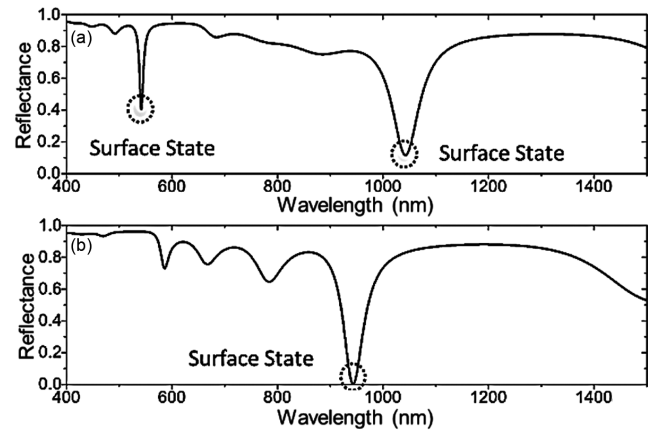


Fig. 6 — (a) TMM Simulated normal incidence reflectance spectrum corresponding to MNG terminated Case-1 PhC design; (b) TMM Simulated normal incidence reflectance spectrum corresponding to MNG terminated Case-2 PhC design.

formation of surface state (at the second-order bandgap) with an MNG-type trivial photonic insulator. Therefore, from the presented simulations and experiments, we observe that the existence/non-existence conditions of surface states turn out to be complementary depending upon whether the PhC termination is being done by the ENG-type or MNG-type trivial photonic insulator.

10 Conclusions

In conclusion, we have experimentally demonstrated the existence of topological edge-like states in 1D PhCs, in commensuration with the canonical SSH model studied in condensed matter systems. Our work demonstrates that unlike the Su-Schrieffer-Heeger model, in case of PhC the topological edge-like states can be volitionally realized with considerable design freedom. Specifically, we have systematically investigated the two possible cases where the PhC has been terminated with ϵ -negative type and μ -negative trivial photonic insulators and observed that the existence conditions for the two scenarios turn out to be complementary. The important aspect to note here is that topological principles facilitate us design freedom in exerting complete control on the very existence of the surface states itself. On the application front, we believe that these controllable surface states can be instrumental in devising novel sources of radiation.

References

- 1 Thouless D J, M Kohmoto, M P Nightingale & M den Nijs, *Phys Rev Lett*, 49 (1982) 405.
- 2 Haldane F D M & S Raghu, *Phys Re Lett*, 100 (2008) 013904.

- 3 Zheng W, Chong Y D, Joannopoulos J D & Soljačić M, *Phys Rev Lett*, 100 (2008): 013905.
- 4 Wang Z, Yidong C, John D J & Marin S, *Nature*, 461 (2009) 772.
- 5 Ozawa T, Hannah M P, Alberto A, Nathan G, Mohammad H, Ling L, Mikael C R, et al. *Rev Mod Phys*, 91 (2019) 015006.
- 6 Lu L, John D J & Marin S, *Nature Photon*, 8 (2014) 821.
- 7 Smirnova D, Daniel L, Yidong C & Yuri K, *Appl Phys Rev*, 7 (2020) 021306.
- 8 Kim M, Zubin J & Junsuk R, *Light: Sci Appl*, 9 (2020) 1.
- 9 Price H, Yidong C, Alexander K, Henning S, Lukas J M, Mark K, Matthias H, et al., *J Phys: Photon*, 4 (2022) 032501.
- 10 Yang Y, Yuichiro Y, Xiongbing Y, Prakash P, Julian W, Baile Z, Masayuki F, Tadao N & Singh R, *Nature Photon*, 14 (2020) 446.
- 11 Slobozhanyuk A, Mousavi S H, Ni X, Smirnova D, Yuri S K & Alexander B K, *Nature Photon*, 11 (2017) 130.
- 12 Xie L C, Wu H C, Jin L & Song Z, *Phys Rev B*, 104 (2021) 165422.
- 13 Gupta N K & Arun M J, Topological photonic systems: Virtuous platforms to study topological quantum matter, arXiv preprint arXiv:2108.05845 (2021).
- 14 Li M, Dmitry Z, Maxim G, Xiang N, Dmitry F, Alexey S, Andrea A & Alexander B K, *Nature Photon*, 14 (2020) 89.
- 15 Ni X, David P, Daria A S, Alexey S, Andrea A & Alexander B K, *Sci Adv*, 4 (2018) 8802.
- 16 Kumar A, Gupta M, Pitchappa P, Wang N, Szriftgiser P, Ducournau G & Singh R, *Nature Commun*, 13 (2022) 1.
- 17 Hassan El, Ashraf F K, Kunst A M, Guillermo A, Emil J B & Mohamed B, *Nature Photon*, 13 (2019) 697.
- 18 Kim M, Zihao W, Yihao Y, Hau T T, Junsuk R & Baile Z, *Nature Commun*, 13 (2022) 1.
- 19 Tan W, Yong S, Hong C & Shun-Qing S, *Sci Rep*, 4 (2014) 1.
- 20 Jin L & Song Z, *Phys Rev B*, 99 (2019) 081103.
- 21 Tan Y J, Wenhao W, Kumar A & Singh R, *Opt Expr*, 30 (2022) 33035.
- 22 Gupta N K & Jayannavar A M, Non-Hermitian Topoelectrical Circuits: Expedient Tools for Topological State Engineering with Gain-Loss Modulation, arXiv preprint arXiv:2108.11587 (2021).
- 23 St-Jean P, Goblot V, Galopin E, Lemaître A, Ozawa T, Gratiet L L, Sagnes I, Bloch J & Amo A, *Nature Photon*, 11 (2017) 651.
- 24 Dikopoltsev Z, Tristan H H, Eran L, Oleg A E, Johannes B, Adriana W, Yaakov L, et al., *Science*, 373 (2021) 1514.
- 25 Yang Z, Eran L, Gal H, Yonatan P, Yaakov L, Miguel A B & Mordechai S, *Phys Rev*, 10 (2020) 011059.
- 26 Su, W P, Schrieffer J R & Heeger A J, *Phys Rev Lett*, 42 (1979) 1698.
- 27 Xiao M, Zhang Z Q & Chan C T, *Phys Rev X*, 4 (2014) 021017.
- 28 Wang Q, Meng X, Hui L, Shining Z & Che T C, *Phys Rev X*, 7 (2017) 031032.
- 29 Gupta N K, Sapireddy S, Tiwari A K, Wanare H & Ramakrishna S A, *Sci Rep*, 12 (2022) 1.
- 30 Yariv A & Pochi Y, *Optical waves in crystals*, New York: Wiley, 5 (1984).
- 31 Gupta N K, Wanare H, Chopra A, Kumar M, Pal S S, Tiwari A K & Ramakrishna S A, Topological Surface State by Hierarchical Concatenation of Photonic Stopbands, In 2022 Workshop on Recent Advances in Photonics (WRAP), *IEEE*, (2022) 1.
- 32 Gupta N K, Kumar M, Tiwari A K, Pal S S, Wanare H & Ramakrishna S A, *Appl Phys Lett*, 121 (2022) 261103.